

## Neutron structural study of a displacively modulated crystal: A soliton regime in betaine calcium chloride dihydrate

O. Hernandez\* and M. Quilichini

*Laboratoire Léon Brillouin (CEA-CNRS), CEA/Saclay, 91191 Gif-sur-Yvette, France*

J. M. Pérez-Mato and F. J. Zúñiga

*Departamento de Física de la Materia Condensada, Facultad de Ciencias, Universidad del País Vasco, Apartado 644,  
48080 Bilbao, Spain*

M. Dušek

*Institute of Physics, Academy of Sciences of the Czech Republic, Cukrovarnická 10, Na Slovance 2, 180 40 Praha 8, Czech Republic*

J.-M. Kiat

*Laboratoire de Structure, Propriétés et Modélisation des Solides (UMR 8580), École Centrale, 92295 Châtenay-Malabry, France  
and Laboratoire Léon Brillouin (CEA-CNRS), CEA/Saclay, 91191 Gif-sur-Yvette, France*

J. M. Ezpeleta

*Departamento de Física Aplicada II, Facultad de Farmacia, Universidad del País Vasco, Apartado 450, 01080 Vitoria-Gasteiz, Spain*

(Received 29 March 1999)

We present a structural study by single-crystal neutron diffraction of the one-dimensional displacively modulated dielectric crystal betaine calcium chloride dihydrate (BCCD). The fourfold and fivefold low-temperature commensurate structures of its Devil's-staircase-type phase diagram have been investigated at 100 and 68 K, respectively. In both structures, the atomic modulation functions, deduced from a four-dimensional refinement, are highly anharmonic. Moreover, the amplitude of the third-order harmonic is as high as  $\approx 30\%$  of that of the first-order harmonic and the phases of the two harmonics are roughly equal. Consequently, many atomic modulation functions display a typical two-step squared shape. On the basis of four-dimensional symmetry arguments, we interpret this modulation anharmonicity as a soliton regime with respect to the lowest-temperature nonmodulated ferroelectric structure. The two-step solution of the sine-Gordon equation can indeed describe at least qualitatively the phase of the modulation for many atoms in BCCD. After the case of thiourea, our work constitutes a complete structural characterization of a soliton regime in an incommensurate system. The physical consequences of this soliton regime in BCCD are discussed. In particular, the relevance of the use of polar Ising pseudospins as a low-temperature structural model is directly established and the theoretical predictions of the double Ising spin model concerning the dielectric anomaly at  $T_s$  are confronted with our results. [S0163-1829(99)02634-X]

### I. INTRODUCTION

Since its synthesis in 1984,<sup>1</sup> betaine calcium chloride dihydrate (BCCD) or  $(\text{CH}_3)_3\text{NCH}_2\text{COOCaCl}_2(\text{H}_2\text{O})_2$  has been studied by many experimental techniques and different theoretical models have been developed in order to explain and to predict its remarkable physical properties.<sup>2</sup> Indeed, this compound constitutes among incommensurate (INC) systems<sup>3</sup> one of the best experimental examples of the Devil's staircase concept:<sup>4</sup> when the temperature decreases at atmospheric pressure, between the high-temperature paraelectric structure (spacegroup  $Pnma$  (Refs. 5,6) with  $a = 10.95$  Å,  $b = 10.15$  Å, and  $c = 10.82$  Å, above  $T_i = 164$  K) and the lowest-temperature nonmodulated ferroelectric structure (spacegroup  $Pn2_1a$ ,<sup>6</sup> below  $T_0 = 46$  K), there is a succession of one-dimensional displacively modulated structures characterized by the wave-vector  $\vec{k} = \delta(T)\vec{c}^*$ , which are either INC (structures INC1 and INC2), or commensurate (mainly  $\delta = \frac{2}{7}, \frac{1}{4}, \frac{1}{5},$  and  $\frac{1}{6}$ ). The dis-

placive transition that occurs at  $T_i$  is driven by a mixed optic-acoustic soft-mode of  $\Lambda_3$  symmetry (antisymmetric for  $C_{2z}$  and  $\sigma_y$ , symmetric for  $E$  and  $\sigma_x$ ).<sup>7,8</sup>

The room-temperature orthorhombic cell contains four formula units of 28 atoms (see Fig. 1 of Ref. 6), among which eight lie on the mirror plane  $\sigma_y$  of the structure, so only 18 atoms are symmetrically independent. This formula unit is composed on one hand of the polar organic betaine molecule  $[(\text{CH}_3)_3\text{N}^+\text{CH}_2\text{COO}^-]$ , and on the other hand of a distorted octahedron  $[\text{CaCl}_2(\text{H}_2\text{O})_2]$  centered on the calcium atom. These two elementary units share an oxygen atom of the carboxyl terminal group of the betaine molecule. The structure can be viewed as a stacking along  $\vec{b}$  of parallel layers at  $y/b = \frac{1}{4}$  and at  $y/b = \frac{3}{4}$ , linked by  $[011]$  diagonal hydrogen bridges ( $\text{Cl} \cdots \text{H}-\text{O}$ ).

The nature of the phase diagram of BCCD is still controversial:<sup>9,10</sup> whereas its low-temperature part is close to a 'harmless' Devil's staircase, several higher-order commensurate structures have been detected in the structure INC2 between the structures  $\delta = \frac{2}{7}$  and  $\delta = \frac{1}{4}$ ,<sup>11,12</sup> which

might indicate, together with a global hysteresis phenomenon of the wave-vector of the modulation,<sup>9</sup> a “complete” Devil’s staircase behavior in this range of temperature. Due to its layer structure and to the nonpolar or polar character along  $\vec{a}$  or  $\vec{b}$  of the different structures of the Devil’s staircase, BCCD displays furthermore very interesting features under pressure or electric field (e.g., structural branching process<sup>13</sup> or unusual dielectric anomalies, for instance the “ $T_s$  anomaly”<sup>14</sup>). This compound is therefore a prototype system for various theoretical models (phenomenological Landau type,<sup>15</sup> semimicroscopic,<sup>16,17</sup> or statistic<sup>18</sup> models).

BCCD has been apparently classified<sup>10</sup> in the so-called Landau type-II INC family,<sup>3</sup> such as thiourea, quartz, or  $\text{NaNO}_2$ : their lowest-temperature structure below  $T_0$  is non-modulated and the Lifshitz invariant in the Landau free-energy density is forbidden; the modulation is assumed to remain nearly sinusoidal even close to  $T_0$ , no soliton regime develops and the transition towards the lowest-temperature nonmodulated structure is always first order.<sup>19</sup> On the other hand, Landau type-I INC systems (e.g., numerous of  $A_2MX_4$  compounds) have a commensurately modulated lowest-temperature structure; the Lifshitz invariant is allowed and a soliton regime is assumed to develop on cooling towards the rather continuous lock-in transition (see Sec. IV B). This Landau rough classification, confirmed by a numerical mean-field analysis,<sup>20</sup> is inconsistent with the case of thiourea: a coexistence of solitonic and sinusoidal modulations has been experimentally detected.<sup>21,22</sup> Recently, this example has been used to prove that the difference between Landau type-I and type-II INC crystals is, as a matter of fact, very schematic.<sup>23,24</sup> In addition, it turns out that BCCD can not be easily classified as a type-II or a type-I INC system. Indeed, even though its lowest-temperature structure is non-modulated, the order parameter describing the sequence of phase transitions is two-dimensional<sup>7,25</sup> (although a simplified phenomenological model based on a one-dimensional order parameter has also been developed,<sup>15</sup>) as in type-I INC compounds. Moreover, unlike other type-II INC crystals, the Lifshitz point in the pressure-temperature phase diagram of BCCD would be very far from the atmospheric pressure [between  $\approx 10$  and  $13$  kbar (Refs. 13,26,27)], or in other words, the temperature region of the modulated structures is very large (around  $118$  K), indicating that BCCD is distinguishable from a typical type-II INC compound (see Refs. 2,14).

The initial motivation of this work is the recent discovery of high-order satellite peaks (mainly of third-order) in a fully deuterated single-crystal of BCCD.<sup>9</sup> Their intensities, measured by neutron diffraction, become below  $T_i - 40 \approx 115$  K (i.e., in the structure  $\frac{7}{2}$ ) clearly consistent with an anharmonic modulation (non-negligible contribution of the third-order harmonic). This result is the first direct experimental evidence of a deviation from the sinusoidal character of the modulation in BCCD, insofar as no high-order satellite peaks have been measured up to now either by  $x$ -ray diffraction,<sup>28–30</sup> or by neutron diffraction.<sup>31</sup> It leads to the two following remarks: (i) from a general viewpoint, the theoretical predictions aforementioned for type-II INC compounds seem to be once more contradicted; (ii) from a particular viewpoint, the previous  $x$ -ray structural study of the structure  $\frac{1}{4}$ ,<sup>30</sup> which has concluded in favor of an harmonic, or almost harmonic, structural model, has to be revised. Ac-

tually, many experimental results in BCCD have been already interpreted assuming a soliton regime,<sup>14,31–34</sup> but a microscopic evidence and an analysis of the nature of this speculated soliton regime were still missing. Consequently, we have studied by means of a four-circle neutron diffraction experiment the two low temperature commensurate structures  $\frac{1}{4}$  and  $\frac{1}{5}$  at  $100$  and  $68$  K, respectively, in order to clarify the situation, i.e., to determine and to interpret the shape of the modulation of the 18 independent atoms of the average structure, or their atomic modulation functions (AMF’s).

The structure of this paper is as follows: first, we describe the experimental method, second, we show that the modulation in BCCD deduced from a four-dimensional (4D) structural refinement is highly anharmonic at least below  $100$  K, third, this low-temperature structural anharmonicity is interpreted on the basis of 4D symmetry arguments as a soliton regime with respect to the lowest-temperature nonmodulated ferroelectric structure. The physical consequences of this soliton regime are then discussed.

## II. EXPERIMENTAL METHOD

The experiment was performed on the four-circle diffractometer 6T2 located on a thermal source at Orphée reactor, Saclay, France. We have used as monochromator crystal pyrolytic graphite vertically bent [reflection  $(0\ 0\ 2)$ , i.e.,  $\lambda = 1.528$  Å]. The cylindrical collimators installed on the primary beam, between the monochromator crystal and the sample, between the sample and the detector, were equal to  $30'$ ,  $15'$ , and  $25'$ , respectively; a pyrolytic graphite filter was mounted on the incident beam in order to reduce higher-order contaminations. The minimum angular resolution was equal to about  $0.2^\circ$ .

The single-crystal of fully deuterated BCCD ( $V \approx 120$  mm<sup>3</sup>) has been grown by slow evaporation from a saturated  $\text{D}_2\text{O}$  solution of completely deuterated pure chemicals (global rate of deuteration equal to 99%). We have previously confirmed<sup>35</sup> that no isotopic effect occurs in BCCD, therefore the deuteration does not disrupt the experiment, but on the contrary it removes the incoherent elastic scattering coming from hydrogen atoms and thus enhances the signal to noise ratio. The sample was hold on the cold finger of a displax closed-cycle cryostat, allowing a thermal stability of  $0.1$  K. The acquisition of the data was performed at  $100$  and  $68$  K for the structures  $\frac{1}{4}$  and  $\frac{1}{5}$ , respectively, over two octants of the reciprocal space by  $\omega$  scans,  $\omega - \theta$  scans, and  $\omega - 2\theta$  scans in the  $2\theta$  range  $0^\circ - 45^\circ$ ,  $45^\circ - 80^\circ$ , and  $80^\circ - 120^\circ$ , respectively.

The stability of standard reflections, including main and superstructure peaks, at  $100$  and  $68$  K, was better than  $1.4\%$ , over  $113$  and  $258$  h, respectively. The cell parameters, refined from the position of 25 and 21 strong main peaks (in the  $\theta$  range  $8.11^\circ - 21.36^\circ$ , and  $14.77^\circ - 21.36^\circ$ , respectively), are  $a = 10.83(2)$  Å,  $b = 9.98(2)$  Å,  $c = 43.13(7)$  Å and  $a = 10.82(3)$  Å,  $b = 9.98(2)$  Å,  $c = 53.93(2)$  Å in the structures  $\frac{1}{4}$  and  $\frac{1}{5}$ , respectively.

The data reduction, realized with the COLL5 program based on the Lehmann and Larsen algorithm,<sup>36</sup> has allowed us to eliminate bad profile principally contaminated by aluminum powder reflections of the cryostat for  $\omega - \theta$  and  $\omega -$

$2\theta$  scans. Finally, 2537 and 5189 reflections have been selected with all observed reflections [i.e., with  $F_{hkl}^2 \geq 3\sigma(F_{hkl}^2)$ ] fulfilling the extinction rules of the space-groups  $P2_1ca$  and  $P2_12_12_1$  for the structures  $\frac{1}{4}$  and  $\frac{1}{5}$ , respectively. These space-groups have been predicted by Pérez-Mato,<sup>7</sup> assuming the same order parameter of  $\Lambda_3$  symmetry for the whole sequence of phase transitions, and for  $P2_1ca$ , yet confirmed by the previous x-ray study.<sup>30</sup> The averaging of the data, considering these space-groups, leads to a number of independent reflections equal to 1737 ( $R_{\text{int}} = 3.68\%$ ) and to 2456 ( $R_{\text{int}} = 3.83\%$ ) for the structures  $\frac{1}{4}$  and  $\frac{1}{5}$ , respectively.

### III. STRUCTURAL REFINEMENT OF THE STRUCTURES $\frac{1}{4}$ AND $\frac{1}{5}$

The two structures investigated are displacively modulated structures, but commensurate ones. Hence, two kinds of structural refinement can be achieved: first, a standard (or 3D) one, i.e., considering the fourfold (with  $4 \times 28 = 112$  independent atoms) and fivefold (with  $5 \times 28 = 140$  independent atoms) commensurate super-cells for the structures  $\frac{1}{4}$  and  $\frac{1}{5}$ , respectively, and using the space-groups aforementioned for each case. Secondly, a 4D one, which uses the superspace description<sup>37</sup> and is based on the average cells  $(a, b, c/4)$  and  $(a, b, c/5)$  for the structures  $\frac{1}{4}$  and  $\frac{1}{5}$ , respectively, plus a modulation wave. The 3D refinements are described elsewhere.<sup>38</sup> In this paper, we shall deal only with the second approach. The main goal is not to decrease the number of refinement parameters,<sup>39,40</sup> but to take into account the modulated nature of these structures and to obtain in a direct manner the shape of the AMF's.

In a one-dimensional displacively modulated structure with a wave vector  $\vec{k}$ , the position of the atom  $\mu$  in the average cell  $\vec{l}$  can be written in the general form

$$\vec{r}(\vec{l}, \mu) = \vec{l} + \vec{r}_0^\mu + \frac{1}{2} \sum_n \vec{u}_n^\mu e^{j2\pi n \vec{k} \cdot (\vec{l} + \vec{r}_0^\mu)}, \quad (1)$$

where  $\vec{r}_0^\mu$  is the average atomic position and  $\vec{u}_n^\mu$  the complex Fourier vectorial amplitudes which fulfil the relation

$$\vec{u}_n^\mu = \vec{u}_{-n}^{\mu*}. \quad (2)$$

We have refined the structures  $\frac{1}{4}$  and  $\frac{1}{5}$  using the package program JANA '96.<sup>41</sup> In this program, the complex Fourier vectorial amplitudes are splitted into their real and imaginary parts, in such a way that the AMF of the atom  $\mu$  along  $i = \vec{a}, \vec{b}$  or  $\vec{c}$  is a function of the internal coordinate  $t$  of the conventional 4D approach<sup>37</sup> [ $t = \vec{k} \cdot (\vec{l} + \vec{r}_0^\mu)$ ] and is given by

$$u^{\mu,i}(t) = \sum_{n=1}^p [u_{n,\text{sin}}^{\mu,i} \sin(2\pi n t) + u_{n,\text{cos}}^{\mu,i} \cos(2\pi n t)],$$

i.e.,

$$u^{\mu,i}(v) = \sum_{n=1}^p \{u_{n,\text{sin}}^{\mu,i} \sin[2\pi n(v + \vec{k} \cdot \vec{r}_0^\mu)] + u_{n,\text{cos}}^{\mu,i} \cos[2\pi n(v + \vec{k} \cdot \vec{r}_0^\mu)]\}, \quad (3)$$

TABLE I. Symmetry operators of the superspace-group  $P(Pnma):(1,s,-1)$  for a wave vector of the modulation  $\vec{k} = \delta(T)\vec{c}^*$  and the internal space origin chosen at the inversion center.

1	$\{E 000,0\}$	5	$\{i 000,0\}$
2	$\left\{C_{2x} \frac{1}{2}\frac{1}{2}, -\frac{\delta}{2}\right\}$	6	$\left\{\sigma_x \frac{1}{2}\frac{1}{2}, -\frac{\delta}{2}\right\}$
3	$\{C_{2y} 0\frac{1}{2}, \frac{1}{2}\}$	7	$\{\sigma_y 0\frac{1}{2}, \frac{1}{2}\}$
4	$\left\{C_{2z} \frac{1}{2}0\frac{1}{2}, -\frac{\delta}{2} + \frac{1}{2}\right\}$	8	$\left\{\sigma_z \frac{1}{2}0\frac{1}{2}, -\frac{\delta}{2} + \frac{1}{2}\right\}$

where the zero-order harmonic is included in  $\vec{r}_0^\mu$ ,  $p$  is the number of harmonics introduced in the refinement,  $v$  is the cell label [ $v = \vec{k} \cdot \vec{l} \pmod{1}$ ] and is related to  $t$  by

$$v = t - \vec{k} \cdot \vec{r}_0^\mu. \quad (4)$$

An alternative and more physical parametrization of the AMF's would be<sup>21</sup>

$$u^{\mu,i}(t) = \sum_{n=1}^p A_n^{\mu,i} \cos[2\pi(nt + \phi_n^{\mu,i})], \quad (5)$$

where  $A_n^{\mu,i}$  and  $\phi_n^{\mu,i}$  are the amplitude and phase of the  $n$ th order harmonic of atom  $\mu$  along  $i = \vec{a}, \vec{b}$ , or  $\vec{c}$ , respectively.

If we consider that the modulated structures  $\frac{1}{4}$  and  $\frac{1}{5}$  derive from the high-temperature INC1 structure (determined at 130 K by Zúñiga *et al.*<sup>29</sup>) and that the order parameter in BCCD corresponds to the irreducible representation  $\Lambda_3$  for the whole sequence of phase transitions, then the superspace-group chosen is  $P(Pnma):(1,s,-1)$ .<sup>7</sup> The symmetry elements of this superspace-group are given in Table I with the following definition:  $\{R|\vec{t}, \tau\}$  is a symmetry operator of the superspace-group,  $R$  is the rotational operation,  $\vec{t}$  is the fractional translation in real space, and  $\tau$  is the translation along the one-dimensional internal space.<sup>39</sup> In general,  $\tau$  depends on the wave vector of the modulation  $\vec{k}$  and also on the origin chosen for the internal coordinates.

Considering two atoms  $\mu$  and  $\nu$  which are related in the average structure by the 3D symmetry operator  $\{R|\vec{t}\}$ , then their  $n$ th-order complex Fourier vectorial amplitudes fulfil<sup>39</sup>

$$\vec{u}_n^\nu = R \vec{u}_{R(R)n}^\mu e^{-j2\pi n \tau_0}, \quad (6)$$

with

$$\tau_0 = \tau + \vec{k} \cdot \vec{t}, \quad (7)$$

and

$$R_f(R) = \pm 1 \quad \text{if} \quad R(\vec{k}) = \pm \vec{k}. \quad (8)$$

If we apply the general rule of Eq. (6) to the particular case of the superspace-group  $P(Pnma):(1,s,-1)$  and to an atom  $\mu$  on special position so that  $\mu = \nu$ , i.e., for BCCD, which lies on the mirror plane  $\{\sigma_y|0\frac{1}{2}, \frac{1}{2}\}$  (case of the eight atoms C1, C3, C4, Ca, D2, N, O1, and O2), then we obtain

TABLE II. Systematic extinction rules of the superspace-group  $P(Pnma):(1,s,-1)$ .

$(0\ k\ 0\ 0): k\ \text{odd}$	$(0\ 0\ l\ m): l+m\ \text{odd}$	$(h\ k\ 0\ 0): h\ \text{odd}$
$(h\ 0\ l\ m): m\ \text{odd}$	$(0\ k\ l\ m): k+l\ \text{odd}$	

the following symmetry restrictions on the sine and cosine amplitudes of the  $n$ th-order harmonics (3) of these atoms:

$$u_{n,\sin}^{\mu,y} = u_{n,\cos}^{\mu,y} = 0 \text{ if } n \text{ even,}$$

$$u_{n,\sin}^{\mu,x} = u_{n,\cos}^{\mu,x} = u_{n,\sin}^{\mu,z} = u_{n,\cos}^{\mu,z} = 0 \text{ if } n \text{ odd.} \quad (9)$$

All these considerations are relevant for the INC structures of BCCD [and indeed, they have been used for the refinement of the INC1 structure at 130 K (Ref. 29)]; no assumption has been made about the rational or irrational value of the misfit parameter  $\delta$ . Precisely, we discuss in the following the three main physical consequences of the commensurate nature,<sup>40,42</sup> of the structures investigated.

(1) Diffraction peaks are superposed (satellite peaks over satellite peaks or over main peaks),<sup>43</sup> and the transformation of the data from a ‘‘commensurate’’ three-index indexation to an ‘‘INC’’ four-index one is not unique. All superposed satellite reflections with different four-index indexation describe equally well the diffraction vector. Usually, when the modulation is sinusoidal or weakly anharmonic, this superposition effect may be neglected, especially if it is a long period commensurate structure. Then, the refinement can be done as if the structure was INC, disregarding the rational value of the wave-vector of the modulation. This procedure, applied in the previous x-ray structural study of the structure  $\frac{1}{4}$ ,<sup>30</sup> is relevant only if high-order satellite peaks are negligible, which is in fact not the case in BCCD below  $T_i$

–40 K  $\approx$  115 K.<sup>9</sup> This point is confirmed by a careful inspection of the present four-circle data in the  $(0\ k\ l)$  scattering plane. In this specific scattering plane, only the satellite peaks belonging to the main reflections with  $k+l=\text{even}$  are not forbidden by the extinction rules of the superspace-group  $P(Pnma):(1,s,-1)$  (see Table II). Consequently, when  $\delta$  is rational, in particular equal to  $\frac{1}{4}$  or to  $\frac{1}{5}$ , between two main reflections along  $\vec{c}^*$  [e.g., between  $(0\ k\ l\ 0)$  and  $(0\ k\ l+1\ 0)$ ,  $l\ \text{even}$ ], the satellite peaks  $(0\ k\ l\ m)$ ,  $m>0$  are not superposed with the satellite peaks  $(0\ k\ l+1\ m)$ ,  $m<0$ , because the latter are extinct. If  $|m|=4$  or 5, satellite peaks  $(0\ k\ l\ m)$ ,  $m>0$  can eventually be superposed with high-order satellite peaks  $(0\ k\ l+2\ -m)$ , but it would concern the same kind of satellite reflections [( $0\ k\ l\ 4$ ) over ( $0\ k\ l+2\ -4$ ) and ( $0\ k\ l\ 5$ ) over ( $0\ k\ l+2\ -5$ ) in the structures  $\frac{1}{4}$  and  $\frac{1}{5}$ , respectively]. Finally, it turns out from this inspection done in both structures that ‘‘pure,’’ or almost ‘‘pure’’ for  $m=4$  or 5, high-order satellite peaks may be very strong, mainly third-order ones, but also fifth-order ones in the structure  $\frac{1}{5}$  [see Fig. 1, where a pseudo- $\vec{Q}$ -scan along  $\vec{c}^*$  between  $(0\ 3\ 5)$  and  $(0\ 3\ 10)$  — in the ‘‘commensurate’’ three-index indexation — is displayed]. The *ad hoc* commensurate option of the program JANA '96,<sup>41</sup> which takes into account this obvious superposition effect of commensurate structures, allows us to overcome this problem.

(2) All the values of the internal coordinate are not relevant, since we can define, unlike the INC case for which the phase of the modulation is not fixed, a commensurate supercell. More specifically to our problem, the values of  $v$  which are relevant, i.e., which correspond to real atomic positions in the structures  $\frac{1}{4}$  ( $\frac{1}{5}$ ) are the 4 (5) values which correspond to 4 (5) consecutive cells:  $v = \Phi + m/4 \pmod{1}$  [ $\Phi + m/5 \pmod{1}$ ],  $m$  integer, therefore only 4 (5) values separated by 0.25 (0.20). The phase  $\Phi$  of the modulation

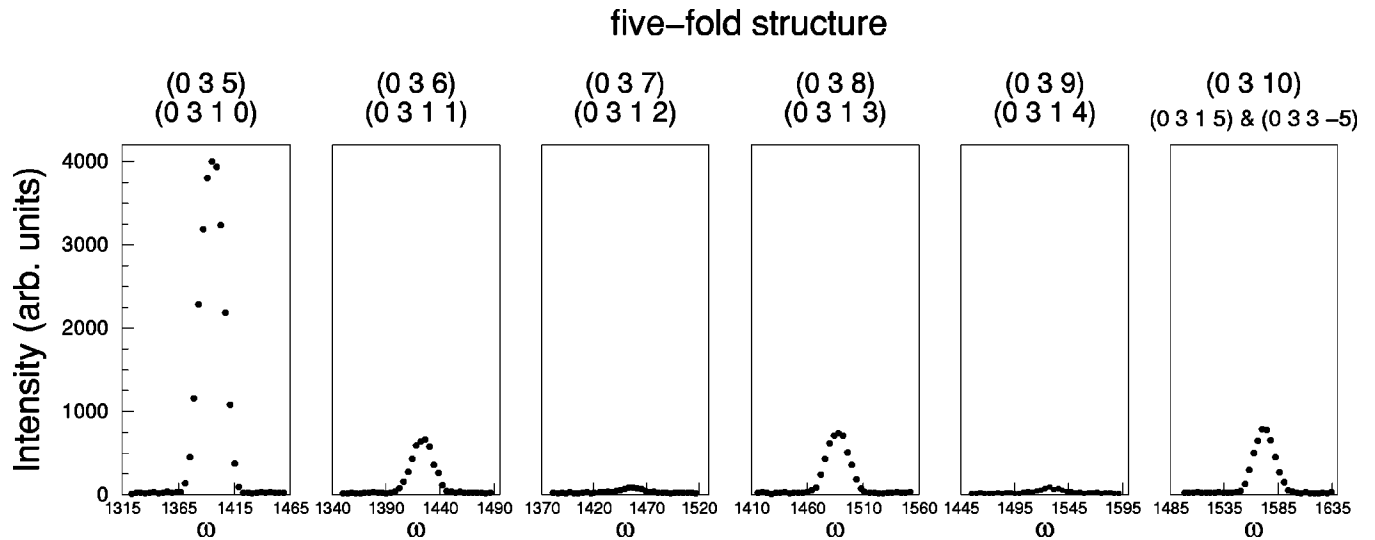


FIG. 1. Pseudo- $\vec{Q}$ -scan along  $\vec{c}^*$  in the fivefold structure at  $T=68$  K between the peaks  $(0\ 3\ 5)$  and  $(0\ 3\ 10)$  — in the ‘‘commensurate’’ three-index indexation — composed of individual  $\omega$  scans. Actually, under the assumption that  $|m|\leq 5$ , and considering the extinction rules of the superspace-group  $P(Pnma):(1,s,-1)$  for  $(0\ k\ l\ m)$  reflections (see Table II), the peaks have been reindexed in the superspace formalism (see Sec. III). Then,  $(0\ 3\ 5)$  becomes a main peak  $(0\ 3\ 1\ 0)$  and two fifth-order satellite peaks, namely,  $(0\ 3\ 1\ 5)$  and  $(0\ 3\ 3\ -5)$ , are superposed at the location of  $(0\ 3\ 10)$ , while the main peak  $(0\ 3\ 2\ 0)$  is extinct by symmetry, this point being corroborated by its almost zero intensity in the fourfold structure where no satellite peaks appear at its position. Notice that odd-order satellite reflections are strong, whereas even-order ones are very weak.



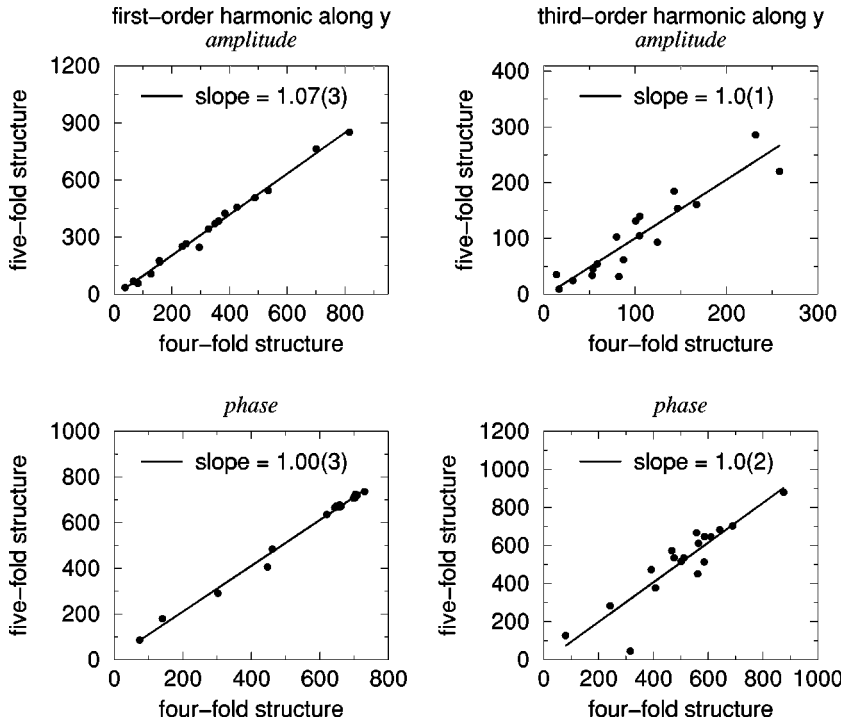


FIG. 2. Amplitude along  $\vec{b}$  (relative units  $\times 10^4$ ) of the first-order harmonic in the structure  $\frac{1}{5}$  versus amplitude along  $\vec{b}$  (relative units  $\times 10^4$ ) of the first-order harmonic in the structure  $\frac{1}{4}$  and phase along  $\vec{b}$  ( $2\pi$  units  $\times 10^3$ ) of the first-order harmonic in the structure  $\frac{1}{5}$  versus phase along  $\vec{b}$  ( $2\pi$  units  $\times 10^3$ ) of the first-order harmonic in the structure  $\frac{1}{4}$  (on the left); Amplitude along  $\vec{b}$  (relative units  $\times 10^4$ ) of the third-order harmonic in the structure  $\frac{1}{5}$  versus amplitude along  $\vec{b}$  (relative units  $\times 10^4$ ) of the third-order harmonic in the structure  $\frac{1}{4}$  and phase along  $\vec{b}$  ( $2\pi$  units  $\times 10^3$ ) of the third-order harmonic in the structure  $\frac{1}{5}$  versus phase along  $\vec{b}$  ( $2\pi$  units  $\times 10^3$ ) of the third-order harmonic in the structure  $\frac{1}{4}$  (on the right). Amplitudes and phases fulfil Eq. (5). ESD's of the slopes (linear fitting) are given in parenthesis.

along the internal space corresponds to cell “0” and defines the selected section of the super-crystal. It is calculated from the following general expression:<sup>40</sup>

$$R_l(R)\Phi - \Phi = \vec{k} \cdot (\vec{t} + \vec{G}) - \tau_4, \quad (10)$$

with  $\tau_4$  being the fourth component of the super-vector  $\vec{\tau}$  after de Wolff *et al.*<sup>44</sup> and  $\vec{G}$  any translational vector of the 3D reciprocal space. If  $R_l(R) = -1$  [the case of the four symmetry elements of the superspace-group  $P(Pnma): (1, s, -1)$  with  $R = C_{2x}, C_{2y}, i$ , and  $\sigma_z$ ], then Eq. (10) should be fulfilled for the operations corresponding to the space group and the proper value of  $\Phi$  can be found. For instance, considering the symmetry element  $\{C_{2x} | \frac{1}{2} \frac{1}{2} \frac{1}{2}, -\delta/2\}$  (for which  $\tau_4 = 0$ ) in the structure  $\frac{1}{4}$ , we obtain  $\Phi = \frac{1}{16} + m'/8$ , with  $m'$  integer. In the structure  $\frac{1}{5}$ , a similar calculation leads to  $\Phi = \frac{1}{20} + m'/10$ , with  $m'$  integer. We have arbitrarily chosen  $m' = 1$ , hence  $\Phi = \frac{3}{16}$  and  $\Phi = \frac{3}{20}$  in the structures  $\frac{1}{4}$  and  $\frac{1}{5}$ , respectively.

(3) The number of positional parameters to be refined (equal to  $3 + 6 \times p$  for an atom in general position), theoretically unlimited in the INC case, cannot exceed  $3 \times 2 \times 4$  and  $3 \times 2 \times 5$  in the structures  $\frac{1}{4}$  and  $\frac{1}{5}$ , respectively. Hence,  $p$  cannot overstep 4 and 5, respectively, but with the fourth and fifth-order harmonics selectively truncated (only sine or cosine component, depending on the value of  $\vec{k} \cdot \vec{r}_0^\mu$  per atom), so as to avoid a refinement artifact which induces nonreasonable interatomic distances along  $t$ .

Finally, taking as starting average structure the room-temperature structural model<sup>6</sup> for both temperatures, and introducing gradually and atom per atom the different harmonics with a strong damping factor, the refinement has converged to the following reliability factors [isotropic extinction of type I (Ref. 45):  $g_{\text{iso}} = 7.5(5)$  and  $7.6(7)$ ; weighting scheme:  $w = 1/[\sigma^2(F_{hkl}) + (un \cdot F_{hkl}^2)]$  with  $un = 2$  and

3% for the structures  $\frac{1}{4}$  and  $\frac{1}{5}$ , respectively]:  $R_{\text{tot}} = 8.25\%$ ,  $R_{\text{main}} = 5.68\%$ ,  $R_{\text{sat1}} = 9.73\%$ ,  $R_{\text{sat2}} = 26.88\%$  (1644, 551, 907, 186 observations, respectively, with 335 positional and 56 thermal parameters) and  $R_{\text{tot}} = 13.11\%$ ,  $R_{\text{main}} = 8.21\%$ ,  $R_{\text{sat1}} = 15.01\%$ ,  $R_{\text{sat2}} = 21.71\%$  (2347, 615, 992, 740 observations, respectively, with 420 positional and 36 thermal parameters) in the structures  $\frac{1}{4}$  and  $\frac{1}{5}$ , respectively. The goodness-of-fit is equal to 4.61 and to 5.68, respectively.<sup>46</sup> No modulation of the thermal parameters can be applied and moreover these latter parameters present two anomalies: (i) they are anisotropic only for some atoms (all the deuterium atoms in the structure  $\frac{1}{4}$ ; only D1, D2, D7, and D8 in the structure  $\frac{1}{5}$ ); (ii) they are slightly negative for the Ca atom in the structure  $\frac{1}{4}$  and for atoms Ca, Cl, C1, C3, C4, N, and O1 in the structure  $\frac{1}{5}$ . The relatively high value of the reliability factors and the correlated thermal parameters anomalies are explained by the relatively low value of  $\sin \theta_{\text{max}}/\lambda$  ( $= 0.567 \text{ \AA}^{-1}$ ) and by the fact that the observed structure factors are truncated in the reciprocal space after data reduction (see Sec. II). Nevertheless, several arguments support the relevance of both structural models. First, the interatomic distances and angles along  $v$  are physically reasonable, i.e., close to those at room temperature,<sup>6</sup> even though in the structure  $\frac{1}{4}$  they are quite different from the ones previously refined from x-ray data,<sup>30</sup> but actually these latter geometric parameters, due to an irradiation effect at constant temperature, are no more relevant (see Sec. V and Refs. 38,47). Secondly, the continuity between the two independent refinements in the structures  $\frac{1}{4}$  and  $\frac{1}{5}$  is very good. This is shown for instance along the direction  $\vec{b}$  of the main atomic displacements with the curves plotting “amplitude (phase) in the fivefold structure versus amplitude (phase) in the fourfold structure” for a given odd-order harmonic (i.e., first- or third-order one) (Fig. 2). Thirdly, the good agreement between the continuous AMF's deduced from these 4D refine-

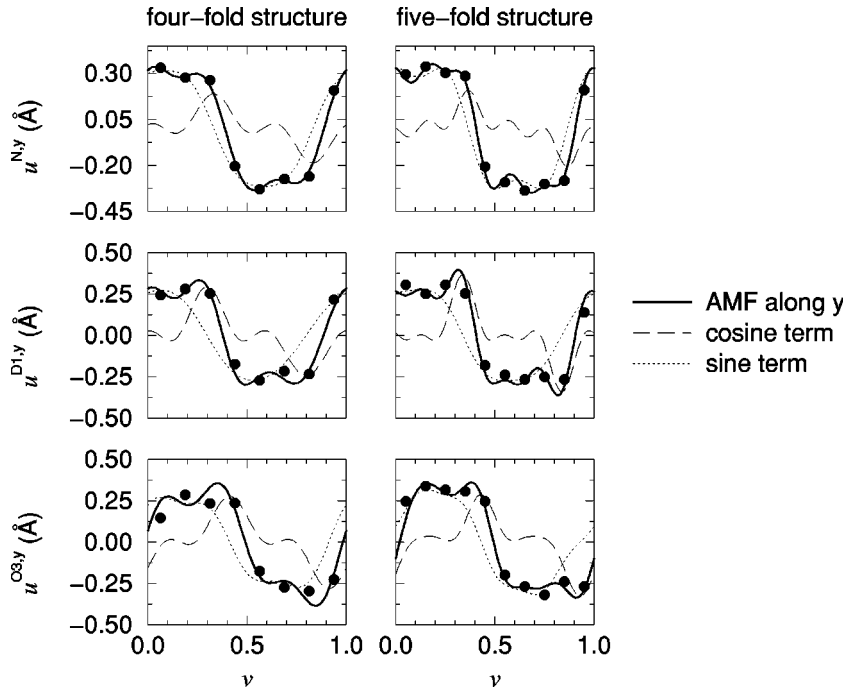


FIG. 3. AMF's along  $\vec{b}$  of atoms N, D1, and O3 from top to bottom, respectively, in the structure  $\frac{1}{4}$  (on the left) and in the structure  $\frac{1}{5}$  (on the right). Black circles indicate real atomic positions along  $v$  as deduced from the 3D refinement (Ref. 38). The sine and cosine splitted terms of the modulation are drawn.

ments and the discrete points deduced from the independent 3D structural models<sup>38</sup> also supports the relevance of the present structural models. This has been evidenced through the procedure described below. The first step is to express the AMF  $u^{\mu,i}(t)$  of an atom  $\mu$  for instance along  $i = \vec{b}$  and in the structure  $\frac{1}{5}$  by taking into account the discrete character of the internal coordinate  $t$  in this commensurately modulated structure. Then, following Eq. (4), where reads as  $v = \Phi + m/5 \pmod{1}$  with the chosen value  $\Phi = \frac{3}{20}$ :

$$u^{\mu}(t) = u^{\mu} \left( \frac{3}{20} + \frac{m}{5} + \vec{k} \cdot \vec{r}_0^{\mu} \right) \equiv u^{\mu}(t_m^{\mu}) = u^{\mu}(\mathbf{v}_m^{\mu} + \vec{k} \cdot \vec{r}_0^{\mu}). \quad (11)$$

Considering the atom  $\nu$  which is related to the atom  $\mu$  in the average structure by the 3D symmetry operator  $\{R|\vec{t}\}$  ( $\{R|\vec{t}, \tau\}$  being an operator of the superspace group), then

$$\vec{r}_0^{\nu} = R\vec{r}_0^{\mu} + \vec{t}, \quad (12)$$

$$\vec{u}^{\nu}(t) = R\vec{u}^{\mu}[R_I^{-1}(t - \tau_0)], \quad (13)$$

with  $\tau_0$  and  $R_I(R)$  defined through Eqs. (7) and (8), respectively. Thus,  $t_m^{\nu} = \mathbf{v}_m^{\nu} + \vec{k} \cdot \vec{r}_0^{\nu} = \mathbf{v}_m^{\nu} + \vec{k} \cdot (R\vec{r}_0^{\mu} + \vec{t}) = \mathbf{v}_m^{\nu} + R\vec{k} \cdot \vec{r}_0^{\mu} + \vec{k} \cdot \vec{t}$  and Eq. (13) along  $i = \vec{b}$  is then written as

$$\begin{aligned} u^{\nu}[t_m^{\nu}] &= R u^{\mu}[R_I^{-1}(t_m^{\nu} - \tau_0)] \\ &= R u^{\mu}[R_I^{-1}(\mathbf{v}_m^{\nu} + R\vec{k} \cdot \vec{r}_0^{\mu} + \vec{k} \cdot \vec{t} - \tau_0)] \end{aligned} \quad (14)$$

$$= R u^{\mu}[\vec{k} \cdot \vec{r}_0^{\mu} + R_I^{-1}(\mathbf{v}_m^{\nu} + \vec{k} \cdot \vec{t} - \tau_0)]. \quad (15)$$

In order to obtain the relation between  $u^{\mu}$  and  $u^{\nu}$ , we calculate the term  $R_I^{-1}(\mathbf{v}_m^{\nu} + \vec{k} \cdot \vec{t} - \tau_0)$  which appears in Eq. (15). More specifically, in the case of a symmetry operation of the superspace-group  $P(Pnma):(1,s,-1)$  that is not retained in

the space-group  $P2_12_12_1$  chosen, e.g.,  $\{\sigma_y|0\frac{1}{2}0,\frac{1}{2}\}$ , for which  $R_I = 1$  and  $\tau_0 = \frac{1}{2}$ , we obtain

$$\begin{aligned} R_I^{-1}(\mathbf{v}_m^{\nu} + \vec{k} \cdot \vec{t} - \tau_0) &= \mathbf{v}_m^{\nu} + 0 - \frac{1}{2} = \frac{3}{20} + \frac{m}{5} - \frac{1}{2} \\ &= \frac{3}{20} + \frac{(m-2)}{5} - \frac{1}{10}, \end{aligned} \quad (16)$$

and finally Eq. (15) can be rewritten

$$u^{\mu} \left( \frac{3}{20} + \frac{(m-2)}{5} - \frac{1}{10} + \vec{k} \cdot \vec{r}_0^{\mu} \right) = R^{-1} u^{\nu} \left( \frac{3}{20} + \frac{m}{5} + \vec{k} \cdot \vec{r}_0^{\nu} \right). \quad (17)$$

To sum up, we have shown that for a symmetry operation  $\{R|\vec{t}, \tau\}$  of the superspace-group that is not retained in the space-group chosen, the AMF of atom  $\mu$  is equal to the AMF of atom  $\nu$ , suitably transformed under  $R^{-1}$ , but at the five positions  $\mathbf{v} = \frac{3}{20} + (m-2)/5 - \frac{1}{10} \pmod{1}$ ,  $m$  integer, namely, at  $\mathbf{v} = 0.05, 0.25, 0.45, 0.65,$  and  $0.85$ , that are different from the five other ‘‘obvious’’ positions defined in point (2) of this section [at  $\mathbf{v} = \frac{3}{20} + m/5 \pmod{1}$ , namely, at  $\mathbf{v} = 0.15, 0.35, 0.55, 0.75,$  and  $0.95$ ]. Hence the comparison between continuous 4D AMF's and the discrete points of the 3D refinement<sup>38</sup> can be done over ten points in the fivefold structure. Notice that if atom  $\mu$  belongs to the mirror plane  $\sigma_y$ , only half of these ten points are independent. Similar arguments lead in the fourfold structure to eight points of comparison between both approaches, with the same symmetry restrictions for atoms belonging to  $\sigma_y$ . As a conclusion, such a comparison is satisfactory as a whole along  $\vec{b}$  (see Fig. 3). Some discrepancy which persists between AMF's and discrete positions for some atoms, mainly in the fivefold structure, can probably be explained by the fact that the 3D refinements have been carried out with geometric soft-

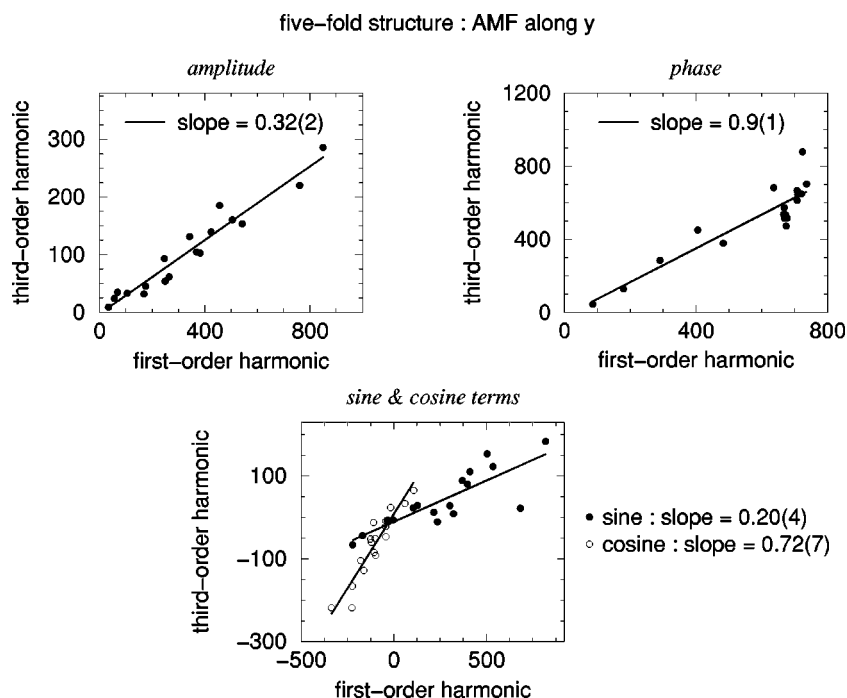


FIG. 4. Amplitude along  $\vec{b}$  (relative units  $\times 10^4$ ) of the third-order harmonic in the structure  $\frac{1}{5}$  versus amplitude along  $\vec{b}$  (relative units  $\times 10^4$ ) of the first-order harmonic in the structure  $\frac{1}{5}$  and phase along  $\vec{b}$  ( $2\pi$  units  $\times 10^3$ ) of the third-order harmonic in the structure  $\frac{1}{5}$  versus phase along  $\vec{b}$  ( $2\pi$  units  $\times 10^3$ ) of the first-order harmonic in the structure  $\frac{1}{5}$  (top). Amplitudes and phases fulfil Eq. (5). Along  $\vec{b}$ , a similar correlation diagram with the splitted sine and cosine partial amplitudes (3) (relative unit  $\times 10^4$ ) is also reported (bottom). ESD's of the slopes (linear fitting) are given in parenthesis.

restraints, relaxed when the convergence was reached,<sup>38</sup> whereas this kind of contrivance has not been used with JANA '96.

#### IV. DISCUSSION

##### A. Description of the low-temperature structural modulation

The  $18 \times 3$  AMF's along  $\vec{a}$ ,  $\vec{b}$ , and  $\vec{c}$  deduced from the aforementioned 4D structural refinements in both structures  $\frac{1}{4}$  and  $\frac{1}{5}$  describe completely the structural modulation for all the atoms of BCCD at 100 and 68 K, respectively.<sup>35</sup> It turns out that, as emphasized above, the continuity between AMF's in the structure  $\frac{1}{4}$  and in the structure  $\frac{1}{5}$  is very good (Fig. 2). It implies that the form of the structural modulation remains essentially unchanged at the phase transition between these two structures and we may assume that this is also true during the structural transitions at lower temperature towards the other modulated structures (with  $\delta = \frac{2}{11}, \frac{1}{6}, \frac{2}{13}, \frac{1}{7}$  etc.), for which there is only a change of period in real space, even though this means that different points in the AMF's become realized as atomic positions in the different structures (see Fig. 3). Then, considering the better refinement quality in the structure  $\frac{1}{4}$  and for the sake of simplicity, we shall discuss in the following the results obtained for this last structure only (nevertheless, the results in the structure  $\frac{1}{5}$  are also reported on Figs. 3–5), which will then be taken as representative of the modulated structure of BCCD in the temperature range 115.3 K (structure  $\frac{1}{4}$ ) – 46 K (nonmodulated ferroelectric structure).<sup>11</sup>

The maximum – minimum atomic displacements along  $v$  with respect to the  $Pnma$  average structure are equal to 0.79 Å (atom D5)–0.05 Å (atom Cl) along  $\vec{b}$ , to 0.45 Å (atom D4)–0.045 Å (atom N) along  $\vec{a}$  and to 0.30 Å (atom D4)–0.007 Å (atom N) along  $\vec{c}$ , respectively. Even though the transverse direction  $\vec{b}$  corresponds to the direction of the main atomic displacements, the contributions along  $\vec{a}$  and  $\vec{c}$

are not negligible, mainly for the methyl group out of the mirror plane  $\sigma_y$  (atoms C2, D3, D4, and D5). Furthermore, let us show how JANA '96 (Ref. 41) has allowed us to analyze the rigid-body behavior along  $v$  of different molecular units. Thus, as soon as the carboxyl group (atoms C4, O1, and O2) is excluded from the rigid molecular unit considered, the total reliability factor becomes remarkably close to the optimal one (with individual atomic modulations:  $R_{\text{tot}} = 8.25\%$ ), i.e., equal to 10.08% for a  $(\text{CD}_3)_3\text{NCD}_2$  rigid group, whereas only isotropic thermal parameters and only three harmonics for the molecular rigid unit are used during this re-refinement of the data. The structural modulation in BCCD can then be described as follows: the terminal part of the betaine molecule, without the carboxyl group, is rigid with respect to the static modulation wave and this molecule describes a frozen libration movement approximately around the bond C3–C4 (almost unmodulated). All the AMF's of atoms belonging to this rigid part of the betaine molecule, including all the deuterium atoms, but also to the the water molecule, are in phase. The carboxyl group is clearly not rigid — as the distorted octahedron centered on the calcium atom — and AMF's along  $\vec{b}$  of atoms O1 and O2 are out of

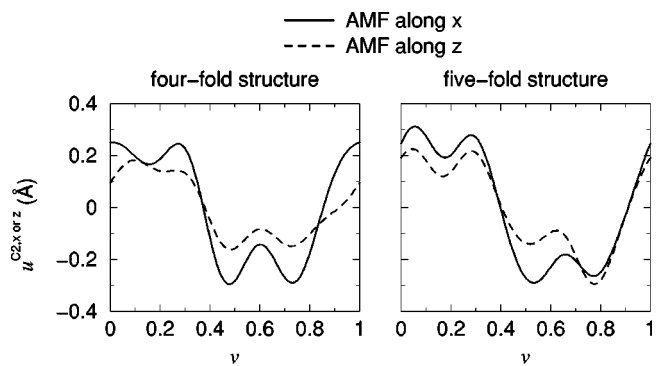


FIG. 5. AMF's along  $\vec{a}$  and  $\vec{c}$  of atom C2: in the structure  $\frac{1}{4}$  (on the left) and in the structure  $\frac{1}{5}$  (on the right).

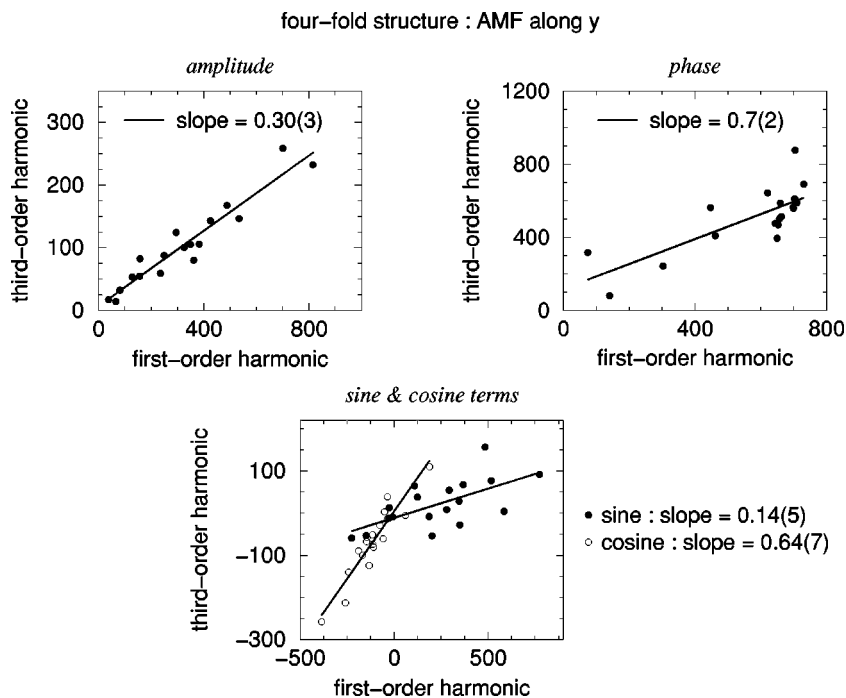


FIG. 6. Amplitude along  $\vec{b}$  (relative units  $\times 10^4$ ) of the third-order harmonic in the structure  $\frac{1}{4}$  versus amplitude along  $\vec{b}$  (relative units  $\times 10^4$ ) of the first-order harmonic in the structure  $\frac{1}{4}$  and phase along  $\vec{b}$  ( $2\pi$  units  $\times 10^3$ ) of the third-order harmonic in the structure  $\frac{1}{4}$  versus phase along  $\vec{b}$  ( $2\pi$  units  $\times 10^3$ ) of the first-order harmonic in the structure  $\frac{1}{4}$  (top). Amplitudes and phases fulfil Eq. (5). Along  $\vec{b}$ , a similar correlation diagram with the splitted sine and cosine partial amplitudes (3) (relative unit  $\times 10^4$ ) is also reported (bottom). ESD's of the slopes (linear fitting) are given in parenthesis.

phase. These results are in agreement with the rigid-body behavior determined from x-ray data in the structure INC1 at 130 K,<sup>29</sup> although in this refinement only one harmonic has been introduced.

The AMF's are all strongly anharmonic (Fig. 3), with a negligible contribution of even-order harmonics (i.e., second-order one in both structures and fourth-order one only in the structure  $\frac{1}{5}$ ) and a strong contribution of the third-order harmonic. The curves “amplitude (phase) of the third-order harmonic versus amplitude (phase) of the first-order harmonic” along one given direction (see top of Fig. 6 along  $\vec{b}$ ) allow us to characterize more quantitatively and in an overall way this anharmonicity of the modulation. The slope  $\times 100$ , deduced from a rather relevant linear fitting of these curves, which gives the global ratio between the amplitudes of the first and third-order harmonics for eighteen atoms along  $\vec{b}$  and only for ten atoms along  $\vec{a}$  (see Sec. III), is equal to 30(3)% and to 33(7)% for the  $\vec{b}$  and  $\vec{a}$  directions, respectively. Along  $\vec{c}$ , this ratio, for only ten atoms (see Sec. III), is equal to 18(10)% but is less relevant because of the high value of the standard error associated with the linear fit. This point results of the very low value of the amplitude of the modulation along  $\vec{c}$  and thus a worse correlation between the different harmonics along this direction. This almost one-third contribution of the third-order harmonic amplitude with respect to the first-order harmonic amplitude is also associated with a particular and “well-adapted” phase relationship between these two harmonics [i.e., their phases, according to Eq. (5), are roughly equal, see top of Fig. 6; notice that the cloud of points around  $10^3 \times \phi_1^{\mu, \vec{b}} \approx 700$  corresponds with the rigid-body part of BCCD] and it induces a typical squared-wave shape of the AMF's along  $\vec{b}$ , but also along  $\vec{c}$  for the methyl group out of the mirror plane (Figs. 3 and 5). However, one should add that this typical two-step squared shape is clearly observed along  $\vec{b}$  only for the atoms belonging to the above-defined rigid part of the betaine molecule and to

the water molecule. Finally, let us emphasize a special feature of the modulation anharmonicity (bottom of Fig. 6): the cosine term of the modulation is almost five times more anharmonic than the sine term [latter global ratio equal to 14(5)% and to 64(7)%, respectively]. This point will be discussed in Sec. V in the scope of the double Ising spin (DIS) model predictions applied to the “ $T_s$  anomaly.”<sup>48</sup>

### B. Interpretation of the structural anharmonicity: a soliton regime in BCCD

In Landau type-I INC family,<sup>20</sup> the “classical” evolution of the structural modulation for decreasing temperature from  $T_i$  down to  $T_0$  is interpreted as the occurrence of a soliton regime precursor of the lock-in transition towards the commensurate lowest-temperature structure.<sup>49,50</sup> This regime is characterized by the growth of high-order harmonics in the distortion, hence by the appearance of odd-order “distortion” satellite peaks in the diffraction pattern.<sup>3</sup> The modulated structure near  $T_0$  is then made of commensurate domains (where the phase of the modulation is constant along  $\nu$ ) of the same symmetry as the lock-in structure, separated by walls or discommensurations or phase solitons, within which the phase of the modulation varies rapidly with  $\nu$  from one constant value to another one, following the nonlinear sine-Gordon equation which is derived from the minimization of the Landau free-energy in the “constant amplitude” assumption.<sup>3</sup> Consequently, the lock-in transition at  $T_0$  is rather continuous, since the commensurate domains grow so that they become macroscopic, or in other words, the distance between discommensurations increases, so that their correlations disappear. The number of steps in the solution of the sine-Gordon equation should correspond to the number of possible different macroscopic domains in the lock-in structure.<sup>51</sup> Our aim is to show that such a behavior occurs in BCCD, too, as in thiourea<sup>23</sup> — a Landau type-II INC system — provided that we take into account the nonmodulated nature of the lowest-temperature “lock-in” structure. There,



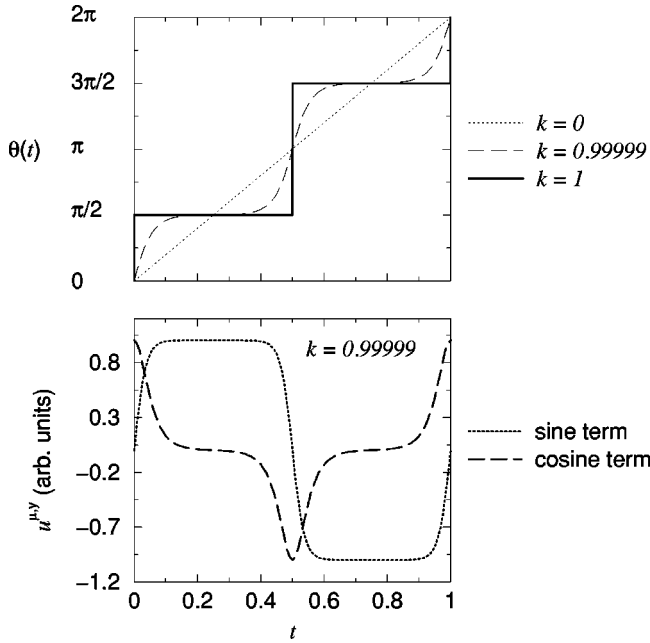


FIG. 7. Phase of the modulation versus the internal coordinate  $t$  calculated from the sine-Gordon equation (31) for  $k=0$ ,  $k=0.99999$ , and  $k=1$ , that correspond to a sinusoidal regime, an intermediate soliton regime and an ideal soliton regime, respectively (top); theoretical AMF along  $\vec{b}$  for  $k=0.99999$  calculated from Eq. (30) (with the assumption that  $e_{B_{3g}}^{\mu,y} = e_{B_{2u}}^{\mu,y}$ ) splitted into its sine and cosine components (bottom).

the number of distinct possible domains is equal to two and corresponds to a ‘lock-in’ phase transition from  $Pnma$  towards  $Pn2_1a$  at  $\vec{q}=\vec{0}$ . Thus, we shall use the two-step solution of the sine-Gordon equation (see top of Fig. 7) as the phase of the modulation without any specific free energy expansion.<sup>24</sup>

Let us calculate the AMF’s along one given main crystallographic direction by applying Eq. (6) to the eight symmetry elements of the superspace-group  $P(Pnma):(1,s,-1)$  (Table I). We have first to calculate the values of  $R_l(R)$  and of  $\tau_0$ , depending on  $R$ :

$$\begin{aligned} R_l(R) &= 1 \quad \text{if } R=E, C_{2z}, \sigma_x \text{ or } \sigma_y, \\ R_l(R) &= -1 \quad \text{if } R=i, C_{2x}, C_{2y} \text{ or } \sigma_z. \end{aligned} \quad (18)$$

Furthermore,

$$\begin{aligned} &\text{if } R=E, i, C_{2x} \text{ or } \sigma_x, \tau_0=0 \text{ and } e^{-j2\pi n\tau_0}=1, \\ &\text{if } R=C_{2y}, \sigma_y, C_{2z} \text{ or } \sigma_z, \tau_0=\frac{1}{2} \text{ and } e^{-j2\pi n\tau_0}=\pm 1 \end{aligned}$$

$$\text{for } n \text{ even and odd, respectively.} \quad (19)$$

Hence, we have now to distinguish the harmonics with respect to their parity. In the case of even-order harmonics, excluding the case  $n=0$ ,

$$\begin{aligned} u_n^v &= Ru_n^\mu \quad \text{if } R=E, \sigma_x, C_{2z} \text{ or } \sigma_y, \\ u_n^v &= -Ru_n^\mu \quad \text{if } R=i, C_{2x}, C_{2y} \text{ or } \sigma_z. \end{aligned} \quad (20)$$

In the case of odd-order harmonics,

$$\begin{aligned} u_n^v &= Ru_n^\mu \quad \text{if } R=E \text{ or } \sigma_x, \\ u_n^v &= -Ru_n^\mu \quad \text{if } R=C_{2z} \text{ or } \sigma_y, \\ u_n^v &= Ru_{-n}^\mu \quad \text{if } R=i \text{ or } C_{2x}, \\ u_n^v &= -Ru_{-n}^\mu \quad \text{if } R=C_{2y} \text{ or } \sigma_z. \end{aligned} \quad (21)$$

If we separate the complex Fourier vectorial amplitudes into their real and imaginary parts, i.e.,

$$u_n^\mu = e_{1,n}^\mu - ie_{2,n}^\mu, \quad (22)$$

where  $e_{1,n}^\mu$  and  $e_{2,n}^\mu$  are equal to the cosine and sine amplitudes of Eq. (3), namely,  $u_{n,\cos}^{\mu,i}$  and  $u_{n,\sin}^{\mu,i}$ , respectively, and considering Eq. (2), Eqs. (20) and (21) give then

$$u_n^\mu = e_{A_g,n}^\mu - ie_{B_{1u},n}^\mu \quad (23)$$

for even-order harmonics, and

$$u_n^\mu = e_{B_{3g},n}^\mu - ie_{B_{2u},n}^\mu \quad (24)$$

for odd-order harmonics, respectively, where  $e_{B_{3g},n}^\mu$ ,  $e_{B_{2u},n}^\mu$ ,  $e_{A_g,n}^\mu$ , and  $e_{B_{1u},n}^\mu$  have the symmetry of  $B_{3g}$ ,  $B_{2u}$ ,  $A_g$ , and  $B_{1u}$ , respectively, which are irreducible representations of  $mmm$ , the point group factor of the space-group  $Pnma$ .

We shall make hereafter several approximations. First, we assume that for a given harmonic parity, the frozen symmetry-modes are roughly the same whatever the order of the harmonic is, then

$$e_{1,n}^\mu = \lambda_n e_{B_{3g}}^\mu \quad \text{and} \quad e_{2,n}^\mu = \lambda'_n e_{B_{2u}}^\mu, \quad (25)$$

if  $n$  odd, and

$$e_{1,n}^\mu = \gamma_n e_{A_g}^\mu \quad \text{and} \quad e_{2,n}^\mu = \gamma'_n e_{B_{1u}}^\mu, \quad (26)$$

if  $n$  even. Thus, Eq. (6) with  $t$  as a variable becomes

$$\begin{aligned} u^\mu(t) &= e_{B_{3g}}^\mu \sum_{\text{odd}} \lambda_n \cos(2\pi nt) + e_{B_{2u}}^\mu \sum_{\text{odd}} \lambda'_n \sin(2\pi nt) \\ &\quad + e_{A_g}^\mu \sum_{\text{even}} \gamma_n \cos(2\pi nt) + e_{B_{1u}}^\mu \sum_{\text{even}} \gamma'_n \sin(2\pi nt), \end{aligned} \quad (27)$$

but as  $\sum_{\text{odd}} \lambda_n \cos(2\pi nt) \propto \sum_{\text{odd}} (\lambda_n e^{i2\pi nt} + \text{c.c.}) = \rho_1(t) e^{i\theta_1(t)} + \text{c.c.}$ , and the three other similar expressions for the three other sums of Eq. (27), then

$$\begin{aligned} u^\mu(t) &= e_{B_{3g}}^\mu \rho_1(t) \cos \theta_1(t) + e_{B_{2u}}^\mu \rho_1'(t) \sin \theta_1'(t), \\ &\quad + e_{A_g}^\mu \rho_2(t) \cos \theta_2(t) + e_{B_{1u}}^\mu \rho_2'(t) \sin \theta_2'(t). \end{aligned} \quad (28)$$

It is now necessary to make a strong assumption, the well-known ‘constant amplitude approximation,’ which implies that  $\rho_1$ ,  $\rho_1'$ ,  $\rho_2$ , and  $\rho_2'$  are independent of  $t$  and that only the phase of the order parameter is spatially inhomogeneous, i.e., dependent of  $t$ . Furthermore, we shall assume that  $\theta_1(t) = \theta_1'(t) = \theta(t)$ ,  $\theta_2(t) = \theta_2'(t) = 2\theta(t)$ , and  $\rho_1 = \rho_1' = \rho_2 = \rho_2'$

=1 by taking into account the over-simple relation  $(\sum_{n \text{ odd}} \lambda_n e^{i2\pi n t})^2 \propto \sum_{n \text{ even}} \gamma_n e^{i2\pi n t} = C^{te} \rho^2 e^{i2\theta(t)}$ , which gives the relation between  $\lambda_n$  and  $\gamma_n$ . Finally, we obtain the following expression for the AMF of an atom  $\mu$ :

$$u^\mu(t) = e_{B_{3g}}^\mu \cos \theta(t) + e_{B_{2u}}^\mu \sin \theta(t) + e_{A_g}^\mu \cos 2\theta(t) + e_{B_{1u}}^\mu \sin 2\theta(t). \quad (29)$$

The last assumption will be to consider an atom  $\mu$  belonging to the mirror plane  $\sigma_y$ , i.e. C1, C3, C4, Ca, D2, N, O1, or O2. In that case, Eq. (9) indicates that only odd-order harmonics will contribute to the modulation along  $\vec{b}$ , the direction of the main atomic displacements, that will be the only direction considered hereafter. Hence, Eq. (29) can be simplified to the following relation:

$$u^{\mu,y}(t) = e_{B_{3g}}^{\mu,y} \cos \theta(t) + e_{B_{2u}}^{\mu,y} \sin \theta(t), \quad (30)$$

where the modulation has been splitted into frozen symmetry modes.

Summing up, the AMF along  $\vec{b}$  of one atom which lies on the mirror plane  $\sigma_y$  is directly equal to a cosine term, which has the symmetry of the  $B_{3g}$  irreducible representation (antisymmetric for  $C_{2z}$ ,  $C_{2y}$ ,  $\sigma_z$ , and  $\sigma_y$ ), plus a sine term, which has the symmetry of the  $B_{2u}$  irreducible representation (antisymmetric for  $C_{2z}$ ,  $C_{2x}$ ,  $i$ , and  $\sigma_y$ ). We propose now to determine the phase  $\theta(t)$  [or  $\theta(v)$ ] of the modulation as a solution of the following sine-Gordon equation adapted to the case of a nonmodulated ‘‘lock-in’’ structure, by only considering general arguments,<sup>52</sup> as emphasized in the introduction of this subsection

$$\left(\frac{d\theta(v)}{dv}\right)^2 = \left(\frac{2K(k)}{\pi}\right)^2 [1 - k^2 \cos^2 \theta(v)], \quad (31)$$

where  $v$  is the cell label,  $k$  is a continuous variable which drives the more or less steplike shape of  $\theta(v)$  and which varies between 0 [sinusoidal regime:  $\theta(v)$  is linear, only one harmonic in the modulation] and 1 [perfect soliton regime: pure two-step shape of  $\theta(v)$ , modulation equal to an infinite sum of  $n$ th odd-order harmonics, with their respective amplitudes equal to  $1/n$  and equal phases], see top of Fig. 7,  $K(k)$  is the complete elliptic integral of the first kind,  $\theta(v+1) = \theta(v) + 2\pi$ . Actually,  $k$  is related to the soliton density  $n_s$ , defined as the ratio ‘‘width of the discommensurations over width of the commensurate domains,’’ by<sup>20</sup>

$$n_s = \frac{\pi}{2K(k)}, \quad (32)$$

thus,  $n_s = 1$  in the sinusoidal regime and  $n_s = 0$  in the perfect soliton regime where the width of the commensurate domains becomes infinite.

The solution  $\theta(t)$  of the sine-Gordon equation (31), calculated numerically, is drawn on the top of Fig. 7 for three values of  $k$ , or of  $n_s$ , namely,  $k=0$  (sinusoidal regime),  $k=0.99999$  (intermediate soliton regime), and  $k=1$  (perfect soliton regime). At the location of the discommensurations [at  $t=0$  and at  $t=0.5 \pmod{1}$ ], the phase  $\theta(t)$  of the modulation is shifted by a value equal to  $\pi$ . The corresponding ‘‘theoretical’’ modulation, determined through Eq. (30) un-

der the simplifying assumption that  $e_{B_{3g}}^{\mu,y} = e_{B_{2u}}^{\mu,y}$  — actually not fully relevant as can be seen on the bottom of Fig. 6 — and splitted into its sine and cosine components, is displayed on the bottom of Fig. 7. It turns out that the global shape of this ‘‘theoretical’’ modulation, assuming implicitly a soliton regime with respect to a nonmodulated structure, is very close to many ‘‘experimental’’ AMF’s (Fig. 3), in particular the AMF’s of atoms belonging to the rigid part of the betaine molecule or to the water molecule. Thus, we have demonstrated that a soliton regime with respect to the lowest-temperature nonmodulated ferroelectric structure occurs in BCCD at low temperature, i.e., strictly speaking below the lock-in transition at  $\delta = \frac{1}{4}$ , but most probably below the plateau at  $\delta = \frac{2}{7}$  (Ref. 9) — in the far lower part of the structure INC1. Correlatively, the splitted cosine and sine terms of the modulation display very specific shapes, that we shall explain below. Indeed, one can observe (bottom of Fig. 7) that the cosine term (symmetry  $B_{3g}$ ) is almost negligible in both commensurate domains, while the sine term (symmetry  $B_{2u}$ ) is predominant there; moreover, the cosine term is confined at the location of the discommensurations. This result is qualitatively in very good agreement with the ‘‘experimental’’ sine and cosine terms of the AMF’s (see Fig. 3), neglecting an offset along  $v$  that is related to the definition of  $v$  (4) and to the value of  $\Phi$  (10). Such an analysis appears also relevant for many other atoms which do not belong to the mirror plane  $\sigma_y$ , as can be seen for instance along  $\vec{b}$  on Fig. 3 for atom D1. This point is explained by the very weak contribution of even-order harmonics to the global distortion, as stressed above. A symmetry-mode analysis performed in the nonmodulated ferroelectric structure<sup>6</sup> has demonstrated that only the  $A_g$  and  $B_{2u}$  frozen modes contribute to the distortion of this structure with respect to the  $Pnma$  basic structure; along  $\vec{b}$ , only the latter contribution is present. So, in BCCD, the structural modulation evolves on cooling towards a soliton regime with respect to the lowest-temperature nonmodulated ferroelectric structure in order to anticipate this structure, which appears from this viewpoint as a ‘‘ground-state’’ energetically more favorable, by confining progressively its contribution of  $B_{3g}$  symmetry, which is forbidden below  $T_0$ , at the location of the discommensurations.

## V. CONCLUDING REMARKS

We have determined by means of single-crystal neutron diffraction the fourfold and fivefold modulated structures of BCCD, at 100 and 68 K, respectively. Both modulations are highly anharmonic, with an almost one-third contribution of the amplitude of the third-order harmonic with respect to the amplitude of the first-order one. Moreover, phases of these two harmonics are roughly equal. As a consequence, the shapes of many AMF’s are very close to a two-step squared function. This structural anharmonicity is interpreted on the basis of four-dimensional symmetry arguments as a soliton regime with respect to the lowest-temperature nonmodulated ferroelectric structure. Indeed, we show that the solution of the sine-Gordon equation adapted to the case of a nonmodulated ‘‘lock-in’’ structure, i.e., with two steps, can describe at least qualitatively the phase of the modulation for

many atoms in BCCD. After the case of thiourea,<sup>21</sup> the present work constitutes a complete structural characterization of a soliton regime in an INC system. In addition, the apparent discrepancy between our results and the previously published x-ray structural analysis of the fourfold structure,<sup>30</sup> where only one harmonic was taken into account, is explained by an irradiation effect at constant temperature:<sup>38,47</sup> in BCCD, an unusual time-variation of the intensity of diffraction peaks occurs under x-ray irradiation, this phenomenon being dramatic for third-order satellite reflections [up to  $-81(3)\%$  after 86 h].

Let us discuss several physical consequences of the present work now. First, we have explained the appearance between the plateaus at  $\delta = \frac{2}{7}$  and  $\delta = \frac{1}{4}$  and the growth on cooling of odd-order satellite peaks<sup>9</sup> by the development of a soliton regime with respect to the lowest-temperature non-modulated ferroelectric structure. The multisolitons regime in BCCD, initially evidenced by EPR,<sup>32,33</sup> indirectly confirmed by dielectric<sup>14,34</sup> or elastic neutron scattering measurements,<sup>31</sup> is therefore fully characterized and explained. It must be stressed that authors of Refs. 31, 32 and 34 have assumed a multisolitons regime precursor of the commensurate structures  $\frac{2}{7}$  or  $\frac{1}{4}$ , in contradiction with our structural results.

Simple symmetry arguments allow us to explain the occurrence of a soliton regime when the temperature decreases down to the transition towards the nonmodulated ferroelectric structure (at  $T_0$ ): the frozen  $B_{3g}$  symmetry-mode of the distortion, which is forbidden below  $T_0$ ,<sup>6</sup> is confined at the location of the discommensurations, and thus progressively reduced for the benefit of the  $B_{2u}$  symmetry-mode, allowed below  $T_0$ . After the case of thiourea,<sup>23</sup> we confirm the generalization of the sine-Gordon equation to all the INC compounds, Landau type-I or type-II, whatever their particular thermodynamic potential is, and correlatively we contradict commonly admitted theoretical results.<sup>19</sup> Furthermore, we confirm at a microscopic level the relevance of the use of polar Ising pseudospins as a low-temperature structural model, as has been implicitly assumed by authors applying

Ising-type or related theoretical models in BCCD.<sup>18</sup> Such a viewpoint is also very useful to explain many dielectric properties of this compound and to interpret new phase transitions under high electric field applied along  $\vec{b}$  without change of the modulation periodicity.<sup>14</sup>

Finally, let us discuss the conclusions deduced from the DIS model concerning the “ $T_s$  anomaly.”<sup>48</sup> At atmospheric pressure, this controversial dielectric anomaly<sup>2</sup> occurs just below the transition towards the fourfold structure.<sup>14</sup> Hence, the present structural model of the fourfold structure, refined from data collected at  $T = 100$  K, corresponds to a structure below  $T_s$ . Neubert *et al.*<sup>48</sup> have predicted *via* the DIS model an “internal” first order transition that would occur in particular in the four-fold structure of BCCD through the flip of four pseudospins belonging to the cosine part of the modulation. This structural change in the pseudo-spins arrangement induces an increase of the solitonic anharmonicity of the cosine part of the modulation below  $T_s$ . Our results corroborate this point (see Sec. IV A and bottom of Fig. 6), but the definitive assignment of this theoretical “internal” transition with the “ $T_s$  anomaly” would actually require to prove that above  $T_s$  the cosine part of the modulation is much more harmonic, but also that the sine part is unchanged in comparison with the situation below  $T_s$ .

#### ACKNOWLEDGMENTS

One of us (O.H.) was financially supported by the “Ministère Français de l’Enseignement Supérieur et de la Recherche.” We want to thank J.-M. Godard (Laboratoire de Physique des Solides, Université Paris XI Paris-Sud, France) for the elaboration of the sample. We are very much indebted to P. Fouilloux for his technical support during the experiment at Orphée reactor. Lastly, we acknowledge Dr. V. Petříček (Institute of Physics, Academy of Sciences of the Czech Republic, Praha, Czech Republic) for his fruitful assistance during the 4D refinement with the program JANA ‘96 and Dr. I. Aramburu (Departamento de Física Aplicada I, Universidad del País Vasco, Bilbao, Spain) for helpful discussions.

\*Present address: Laboratoire de Dynamique et Structure des Matériaux Moléculaires (UPRESA au CNRS 8024), UFR de Physique, Bâtiment P5, Université des Sciences et Technologies de Lille, 59655 Villeneuve d’Ascq, France.

<sup>1</sup>H.J. Rother, J. Albers, and A. Klöpperpieper, *Ferroelectrics* **78**, 3 (1984).

<sup>2</sup>G. Schaack and M. le Maire, *Ferroelectrics* **208-209**, 1 (1998).

<sup>3</sup>H.Z. Cummins, *Phys. Rep.* **185**, 211 (1990).

<sup>4</sup>S. Aubry, *Physica D* **7**, 240 (1983).

<sup>5</sup>W. Brill, W. Schildkamp, and J. Spilker, *Z. Kristallogr.* **172**, 281 (1985).

<sup>6</sup>J.M. Ezpeleta, F.J. Zúñiga, W. Paulus, A. Cousson, J. Hlinka, and M. Quilichini, *Acta Crystallogr., Sect. B: Struct. Sci.* **52**, 810 (1996).

<sup>7</sup>J.M. Pérez-Mato, *Solid State Commun.* **67**, 1145 (1988).

<sup>8</sup>J. Hlinka, M. Quilichini, R. Currat, and J.-F. Legrand, *J. Phys.: Condens. Matter* **8**, 8207 (1996).

<sup>9</sup>O. Hernandez, J. Hlinka, and M. Quilichini, *J. Phys. I* **6**, 231 (1996).

<sup>10</sup>G. Schaack, M. le Maire, M. Schmitt-Lewen, M. Illing, A. Len-

gel, M. Manger, and R. Straub, *Ferroelectrics* **183**, 205 (1996).

<sup>11</sup>H.G. Unruh, F. Hero, and V. Dvořák, *Solid State Commun.* **70**, 403 (1989).

<sup>12</sup>S.A. Sveleba, V. Kapustianik, J. Polovinko, M. Bublik, R. Strykowiec, and Z. Czaplá, *Phys. Status Solidi A* **147**, 257 (1995).

<sup>13</sup>R. Ao, G. Schaack, M. Schmitt, and M. Zöller, *Phys. Rev. Lett.* **62**, 183 (1989).

<sup>14</sup>M. le Maire, R. Straub, and G. Schaack, *Phys. Rev. B* **56**, 134 (1997).

<sup>15</sup>J.L. Ribeiro, J.-C. Tolédano, M.R. Chaves, A. Almeida, H.E. Müser, J. Albers, and A. Klöpperpieper, *Phys. Rev. B* **41**, 2343 (1990).

<sup>16</sup>C. Kappler and M.B. Walker, *Phys. Rev. B* **48**, 5902 (1993).

<sup>17</sup>J. Hlinka, M. Quilichini, R. Currat, and J.-F. Legrand, *J. Phys.: Condens. Matter* **8**, 8221 (1996).

<sup>18</sup>B. Neubert, M. Pleimling, and R. Siems, *Ferroelectrics* **208-209**, 141 (1998).

<sup>19</sup>R.A. Cowley and A.D. Bruce, *Adv. Phys.* **29**, 1 (1980).

- <sup>20</sup>A.D. Bruce, R.A. Cowley, and A.F. Murray, *J. Phys. C* **11**, 3591 (1978).
- <sup>21</sup>F.J. Zúñiga, G. Madariaga, W.A. Paciorek, J.M. Pérez-Mato, J.M. Ezpeleta, and I. Etxebarria, *Acta Crystallogr., Sect. B: Struct. Sci.* **45**, 566 (1989).
- <sup>22</sup>S. Tanisaki, H. Mashiyama, and K. Hasebe, *Acta Crystallogr., Sect. B: Struct. Sci.* **44**, 441 (1988).
- <sup>23</sup>I. Aramburu, G. Madariaga, and J.M. Pérez-Mato, *Phys. Rev. B* **49**, 802 (1994).
- <sup>24</sup>I. Aramburu, G. Madariaga, and J.M. Pérez-Mato, *J. Phys.: Condens. Matter* **7**, 6187 (1995).
- <sup>25</sup>J.L. Ribeiro, M.R. Chaves, A. Almeida, J. Albers, A. Klöpperpieper, and H.E. Müser, *J. Phys.: Condens. Matter* **1**, 8011 (1989).
- <sup>26</sup>R. Siems and T. Tentrup, *Ferroelectrics* **98**, 303 (1989).
- <sup>27</sup>M.R. Chaves, A. Almeida, J.-M. Kiat, J.-C. Tolédano, J. Schneck, R. Glass, W. Schwarz, J.L. Ribeiro, A. Klöpperpieper, and J. Albers, *Phys. Status Solidi B* **189**, 97 (1995).
- <sup>28</sup>W. Brill and K.H. Ehses, *Jpn. J. Appl. Phys., Suppl.* **24**, 826 (1985).
- <sup>29</sup>F.J. Zúñiga, J.M. Ezpeleta, J.M. Pérez-Mato, W. Paciorek, and G. Madariaga, *Phase Transit.* **31**, 29 (1991).
- <sup>30</sup>J.M. Ezpeleta, F.J. Zúñiga, J.M. Pérez-Mato, W. Paciorek, and T. Breczewski, *Acta Crystallogr., Sect. B: Struct. Sci.* **48**, 261 (1992).
- <sup>31</sup>A. Almeida, M.R. Chaves, J.-M. Kiat, J. Schneck, W. Schwarz, J.-C. Tolédano, J.L. Ribeiro, A. Klöpperpieper, H.E. Müser, and J. Albers, *Phys. Rev. B* **45**, 9576 (1992).
- <sup>32</sup>J.L. Ribeiro, J.-C. Fayet, J. Emery, M. Pézeril, J. Albers, A. Klöpperpieper, A. Almeida, and M.R. Chaves, *J. Phys. (France)* **49**, 813 (1988).
- <sup>33</sup>M. Fujimoto and Y. Kotake, *J. Chem. Phys.* **90**, 532 (1989).
- <sup>34</sup>M.R. Chaves, A. Almeida, J.L. Ribeiro, P. Simeão Carvalho, J.-C. Tolédano, J. Schneck, J.-M. Kiat, W. Schwarz, H.E. Müser, A. Klöpperpieper, and J. Albers, *Ferroelectrics* **125**, 81 (1992).
- <sup>35</sup>O. Hernandez, Ph.D. thesis, Université Pierre et Marie Curie (Paris VI), France, 1997.
- <sup>36</sup>M.S. Lehmann and F.K. Larsen, *Acta Crystallogr., Sect. A: Cryst. Phys., Diffr., Theor. Gen. Crystallogr.* **30**, 580 (1974).
- <sup>37</sup>T. Janssen and A. Janner, *Adv. Phys.* **36**, 519 (1987).
- <sup>38</sup>O. Hernandez, J.-M. Kiat, A. Cousson, W. Paulus, J. M. Ezpeleta, and F. J. Zúñiga, *Acta Crystallogr., Sect. C: Cryst. Struct. Commun.* (to be published).
- <sup>39</sup>J.M. Pérez-Mato, G. Madariaga, F.J. Zúñiga, and A. Garcia Arribas, *Acta Crystallogr., Sect. A: Found. Crystallogr.* **43**, 216 (1987).
- <sup>40</sup>J. M. Pérez-Mato, in *Methods of Structural Analysis of Modulated Structures and Quasicrystals*, edited by J. M. Pérez-Mato, F. J. Zúñiga, and G. Madariaga (World Scientific, Singapore, 1991) p. 117.
- <sup>41</sup>V. Petříček and M. Dušek, *JANA '96: System for Structure Analysis and Refinement of Modulated and Composite Structures* (Institute of Physics ASCR, Praha, Czech Republic, 1996).
- <sup>42</sup>S. van Smaalen, *Acta Crystallogr., Sect. A: Found. Crystallogr.* **43**, 202 (1987).
- <sup>43</sup>A. Yamamoto, *Acta Crystallogr., Sect. A: Found. Crystallogr.* **38**, 87 (1982).
- <sup>44</sup>P.M. de Wolff, T. Janssen, and A. Janner, *Acta Crystallogr., Sect. A: Found. Crystallogr.* **37**, 625 (1981).
- <sup>45</sup>P. Becker and P. Coppens, *Acta Crystallogr., Sect. A: Found. Crystallogr.* **30**, 129 (1974).
- <sup>46</sup>The final atomic parameters at 100 and 68 K, i.e., the average structure and the AMF's, can be obtained from the authors.
- <sup>47</sup>O. Hernandez, J. M. Ezpeleta, J. M. Pérez-Mato, G. Madariaga, M. Quilichini, F. J. Zúñiga, and T. Breczewski (unpublished).
- <sup>48</sup>B. Neubert, M. Pleimling, and R. Siems, *J. Phys.: Condens. Matter* **10**, 6883 (1998).
- <sup>49</sup>W.L. Mac Millan, *Phys. Rev. B* **14**, 1496 (1976).
- <sup>50</sup>P. Bak and V.J. Emery, *Phys. Rev. Lett.* **36**, 978 (1976).
- <sup>51</sup>J.M. Pérez-Mato and G. Madariaga, *Solid State Commun.* **58**, 105 (1986).
- <sup>52</sup>I. Aramburu, G. Madariaga, J.M. Pérez-Mato, and T. Breczewski, *Acta Crystallogr., Sect. A: Found. Crystallogr.* **52**, 203 (1996).